Available online at www.sciencedirect.com
SCIENCE DIRECT®
Deep-Sea Research I 51 (2004) 1347–1366
DEEP-SEA RESEARCH PART I
www.elsevier.com/locate/dsr

The Bering Strait's grip on the northern hemisphere climate

Agatha M. De Boer[a,b], Doron Nof[a,c,*]

[a] Department of Oceanography, Florida State University, 4320, Tallahassee, FL 32306-4320, USA
[b] Atmospheric and Oceanic Sciences Program, GFDL, Princeton University, P.O. Box 308, Princeton, 08540, USA
[c] Geophysical Fluid Dynamics Institute, Florida State University, FL, USA

Received 23 December 2002; received in revised form 18 March 2004; accepted 20 May 2004

Abstract

The last 10,000 years have been characterized by distinctly stable climates. For the earlier glacial period (up to 125,000 years ago), climate records show long-lasting large-amplitude oscillations, generally known as Dansgaard–Oeschger (D/O) or Heinrich events. These fluctuations are believed to be a result of freshwater anomalies in the North Atlantic which dramatically reduce the transport of the meridional overturning cell (MOC). They are followed by a recovery of the MOC. Here, we propose that such long lasting instabilities in the meridional circulation are only possible during glacial periods when the Bering Strait (BS) is closed. An analytical ocean model which includes both wind and thermohaline processes) is used to show that, during interglacial periods (when the BS is open) perturbations in North Atlantic Deep Water (NADW) formation are quickly damped out. This new mechanism involves the strong winds in the Southern Ocean (SO) which, with an open BS, quickly [O(1–10 years)] flush any large low salinity anomalies out of the Atlantic and into the Pacific Ocean. During glacial periods, the stabilizing effect is prevented by the closure of the BS which traps the anomalies within the Atlantic, causing long lasting perturbations. We also show that no continuous fresh-water flux is needed in order to keep the collapsed MOC from a recovery in the closed basin case, but a relatively large continuous flux of 0.19 Sv is required in order to keep the collapsed state in the open BS case. With a smaller freshwater transport, the open MOC quickly recovers. This also indicates that an open BS is more stable than the closed BS case. Process-oriented numerical simulations using idealized geometry in a two-layer ocean support our analytical solutions and show that the flushing mechanism is active even when the shallow BS sill is included.
© 2004 Elsevier Ltd. All rights reserved.

Keywords: North Atlantic; Bering Strait; Southern Ocean winds; Thermohaline; Interglacial climate stability

1. Introduction

The North Atlantic (NA) is an integral part of the Earth's heat engine. Here, warm surface water is transformed to deep water by releasing great quantities of heat to the atmosphere. This flow surfaces outside the Atlantic Ocean and

*Corresponding author. Department of Oceanography, Florida State University, 4320, Tallahassee, FL 32306-4320, USA. Tel.: +1-850-644-2736; fax: +1-850-644-2581.
E-mail address: nof@ocean.fsu.edu (D. Nof).

0967-0637/$ - see front matter © 2004 Elsevier Ltd. All rights reserved.
doi:10.1016/j.dsr.2004.05.003

re-enters the Atlantic from the south. The cycle is known as the ocean's meridional overturning cell (MOC).

Because of its associated heat transport, reorganizations of the MOC cell have often been suggested (Boyle, 2000; Marotzke, 2000; Clark et al., 2002) as the cause of the multiple climate fluctuations during the last glacial period, also known as Dansgaard–Oescheger D/O events (Bond et al., 1993; Blunier et al., 1998; Labeyrie, 2000). These millennial-scale cycles (Fig. 1) are generally believed to be a result of freshwater anomalies in the NA. Some of the cold peaks in the Greenland record can be traced directly to massive ice sheets discharges called Heinrich events (Broecker, 1994; Cacho et al., 1999; Bard et al., 2000; Bard, 2002). The accompanying salinity anomaly renders the surface water too fresh for deep convection (Birchfield et al., 1994; Saravanan and McWilliams, 1995; Stocker, 2000; Ganopolski and Rahmstorf, 2001, 2002; Schmittner et al., 2002).

Curiously enough, such high amplitude oscillations have been absent during the Holocene (see again Fig. 1) and evidence is mounting that the penultimate interglacial was equally stable (Kukla, 2000; Adkins et al., 1997; Rioual et al., 2001; Shemesh et al., 2001). We propose here that the switch between stable and unstable climates is the *onset and cessation of flow through the Bering Strait* (*BS*) as modulated by sea level variations. We suggest that this opening took place abruptly (relative to the slow sea level rise) due to an initial jamming of the strait by icebergs and broken ice sheets. We speculate that such jamming was created by the funnel-like shape of the adjacent continent. It persisted until the size of the icebergs was reduced to a size that could pass through the strait, and the sea level difference between the Arctic and Pacific rose to a level high enough to break the dam. Such a scenario is not unusual. It has been argued that Lake Agassiz was dammed in a similar fashion and that icebergs also jammed the Denmark Straits.

Our model does not only explain observed data. It also helps in the interpretation of coupled numerical models which suggest that global-warming-induced precipitation increase and glacier melt may inhibit NADW formation and thereby halt the overturning circulation (Manabe and Stouffer, 1993; Stocker, 1997). The results and details here are an extension of the brief

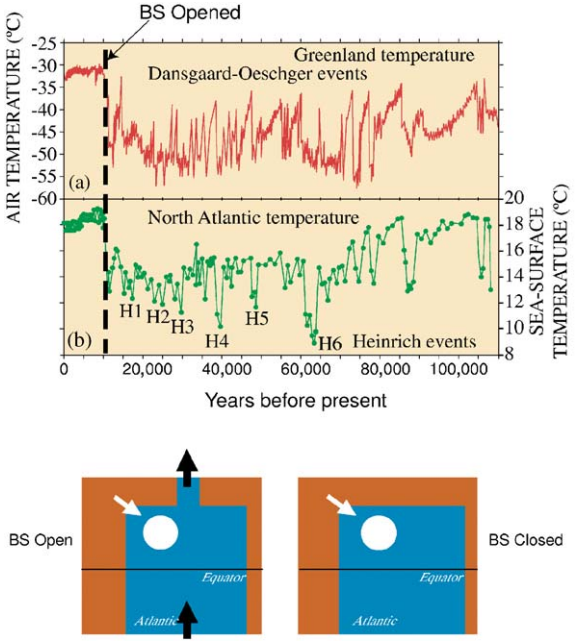

Fig. 1. (Top) (a,b) Atmospheric temperature record obtained from the Greenland GIPS2 ice core (upper panel). Note that, prior to the opening of the BS, large ice sheets and their induced albedo kept the mean temperature lower than it is today. The NA sea surface temperature record displays a very similar structure (lower panel). Six Heinrich events (cool NA temperature periods which correspond to massive ice sheet discharges) are indicated by H1–H6. The occurrence of high amplitude rapid oscillations decreased notably after the opening of the BS, 10.4 ka BP. We argue that, although the meridional overturning cell (MOC) recovers from a freshwater-induced collapse in both the open and closed BS cases, the recovery in the open BS case is much quicker than that in the closed case. This is related to our proposed BS flushing mechanism which explains the very small temperature fluctuations during the last 10,000 years compared to the large fluctuations in the period prior to that. (adapted from Bard, 2002). (Bottom) Schematic diagram of our proposed flushing mechanism. During glacial periods (low sea level) the BS is closed and any ice-induced freshwater perturbations in the North Atlantic stay trapped there (right panel). Ultimately (within 100 years or so), dissipation via diffusion and evaporation causes the MOC to recover. On the other hand, during interglacial periods (high sea level), the strong southern winds quickly flush any fresh anomalies out of the Atlantic via the open strait which acts like an open exhaust valve. Hence, in the open BS case, the MOC quickly recovers.

communication of De Boer and Nof (2004). No new models are introduced here; rather, we present a detailed description of the models that lead to the main outcome described in the above referenced "letter".

The essence of our proposed scenario is as follows. Island rule calculations show that, with an open BS and no NADW formation, 4 Sv(1 Sv = 10^6 m^3/s) of upper ocean water would be forced by the strong SO winds into the South Atlantic (SA). One can think of this flow as being the result of a strong Ekman flux in the SO. This 4 Sv will exit the NA via the Arctic and the open BS and flow into the Pacific (Fig. 2) implying that any ice-sheet-induced freshwater anomalies in the NA would be vigorously flushed out of the NA within several years. The implication is that any freshwater perturbation (such as a Heinrich event) which is strong enough to completely shut off the NADW formation, would be quickly flushed out of the NA and into the Pacific. Consequently, the NADW formation will immediately (i.e., within several years) resume.

On the other hand, when the BS is closed, freshwater perturbations (due to Heinrich or other events involving salinity anomalies) are trapped in the NA. The ocean ultimately recovers also from these perturbations but this recovery is achieved (and the anomaly eliminated) via processes such as diffusion or evaporation which are much slower (50–1000 years). We shall argue that our new BS flushing mechanism is responsible for the very small temperature fluctuations during the Holocene. It is important to realize that our mechanism is associated with the dynamical role of the BS rather than with the familiar BS buoyancy flux. Recall that the buoyancy flux involves merely the flux of, say, a salinity anomaly through the strait ($Q \times S$, where Q is the mass flux and S is the salinity anomaly). An analysis involving the buoyancy flux alone considers the strait to be *physically closed*. Hence, it completely ignores the effect that the mass flux (going through the BS) has on the NA circulation and essentially filters out our proposed flushing mechanism. What we refer to as the *dynamical role* is the effect of such flushing and we shall argue that this effect is very dramatic.

1.1. Background

Observations support the idea of a dynamical BS control on climate stability. Since the last glacial maximum, 19 ka BP (kilo annum before present), global sea level has risen by 130 m (Yokoyama et al., 2000). The BS, being presently only 45 m deep opened up to flow around 10.4 ka BP (Dyke et al., 1996) which is coincident with the onset of the stable Holocene. Also, it is reasonable to assume that the BS was open during the height of the last interglacial, ~125 ka BP, when the global level was 7 m higher than today (Johnson, 2001). Although the stability of the last interglacial is still a matter of debate, recent studies favor the idea that it was a stable climatic period (Adkins et al., 1997; Kukla, 2000; Rioual et al., 2001; Shemesh et al., 2001). Correlating the BS through flow and climate stability for the intervening period (~40–110 ka BP) is not feasible, because the sea level history at the strait is unknown. Uncertainties exist in both the eustatic, or global, component (Chappell and Shackleton, 1986; Shackleton, 1987; Chappell et al., 1996) and the isostatic component, i.e., the local response of the mantle due to shifts in surface weight (Lambeck and Chappell, 2001).

In the Atlantic Ocean there is an excess of evaporation over precipitation and a steady state is maintained in part by the return of freshwater from the Pacific to the Atlantic through the BS. There are also compensations through the AAIW and AABW (which will be indirectly included in our model). Recently, studies using ocean general circulation models (Goosse et al., 1997; Hasumi, 2002) indicate that NADW formation is reduced by the BS through flow. Shaffer and Bendtsen (1994) employed a 3-box model with a geostrophically controlled BS flow (which is proportional to the depth of the sill in the BS) to show that the overturning could be arrested if the sea level is high enough to force a sufficient flow through the BS. As the sea level increases, their model shifts from a regime in which both an operational and an arrested overturning can exist, to a regime which cannot sustain any overturning. They argued, therefore, that the higher sea level of the last interglacial could explain some of the proxies that

indicate a more unstable interglacial (Dansgaard et al., 1993). Our work differs from the above studies in that we do not merely assume a geostrophically controlled BS through flow, but rather, determine the flow from the *global* wind field and the rate of NADW formation.

Another model of the influence of the BS freshwater flux is that of Weijer et al. (2000). They used a two-dimensional numerical model of the Atlantic overturning, to show that, via its buoyancy flux, the BS tends to destabilize the overturning. Our work differs from that of Weijer et al. (2000) in that, as just mentioned, we also consider the dynamical effect of the strait and not only its buoyancy flux. We shall argue that the dynamical effect is more important than the buoyancy flux effect because it allows the NA to be flushed by a wind-induced flow. Related studies concerning the effect of freshwater on the thermohaline circulation are that of Nilsson and Walin (2001), Keeling (2002) and Tziperman and Gildor (2002).

It is appropriate to note here in passing that, although the first opening of the BS (Marincovich and Gladenkov, 1999) and the uplift of the Panama Isthmus (Haug and Tiedemann, 1998; Nof and Van Gorder, 2003) had major impacts on the ocean circulation, our study pertains only to the sea level-induced openings and closures of the BS during the late Quaternary (last ~ 1 million years).

Overall, most of the previous studies suggest that more flow through the BS results in instability of the NADW formation process, i.e., the BS tends to destabilize the MOC due to its freshening effects. Here, we shall argue that, under some conditions, such as when low salinity perturbations in the NA are considered, the opposite is true—the BS stabilizes the MOC.

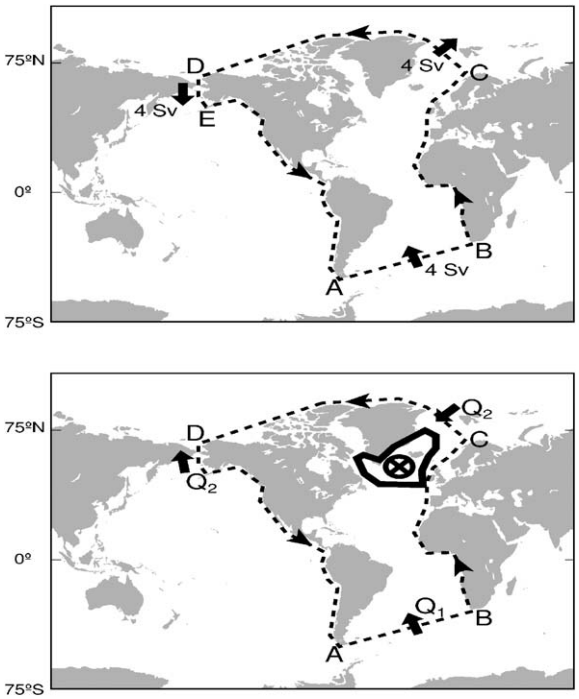

Fig. 2. (Top panel) Island rule calculation of the no-NADW formation open BS geography. The integration is done in a counterclockwise manner along the dashed line. It indicates that, in the absence of NADW formation, 4 Sv (of upper ocean water) would be forced into the SA. This 4 Sv, which is primarily due to the strong SO winds, would exit the NA through cross-section CD and then through the Arctic and the open BS. Note that 60% of the transport is due to the strong SO winds acting on AB. The winds over the Arctic and North Atlantic are so weak compared to the SO winds that altering the integration path in the Arctic virtually makes no difference at all. (Lower panel) Island rule calculation for the North Atlantic with NADW formation. Q_1 and Q_2 are the transports into the Atlantic from the south and north, respectively. The convection region in the NA (whose upper layer volume is M) is outlined in solid black and sinking is indicated by $\otimes$. Note that the direction of the flow through the BS reverses when the NADW formation ceases.

1.2. Present approach

We introduce a novel analytical approach, which considers not only the buoyancy effect of BS freshwater flux on NADW formation, but also the important dynamical effect of the strong SO winds and their induced flow through the BS. The NA, between 50°N and 70°N (Figs. 2 and 3), is regarded as a mixed box which receives salty water from the South Atlantic (SA) and freshwater from the Pacific through the BS. The inflows are determined by the wind field and the overturning rate, and deep water is formed in accordance to the salinity of the box (Section 2). We use this model to argue that the striking correlation between the opening of the BS (10.4 ka BP) and the onset of climate stability (Fig. 1) is not merely a coincidence, but rather a causal relation.

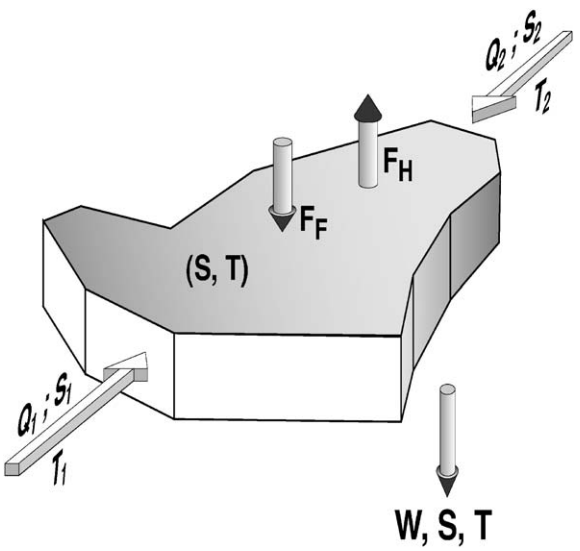

Fig. 3. A three-dimensional view of the (mixed) dynamical-box model of the NA between 50°N and 70°N (i.e., the box bounded by the solid black contour in Fig. 2). The salinity and temperature of the NA box (S and T) are determined by the salinities S_1 and S_2 and temperatures T_1 and T_2 of the water flowing in from the SA (Q_1) and the Arctic/Pacific (Q_2) as well as by the surface freshwater flux, F_F and the heat flux, F_H.

In Section 3, we discuss how, during interglacials, the ocean recovers almost instantly (i.e., within several years or less) from a large perturbation that is sufficient to shut down the overturning. We show that anomalies in the NA surface salinity (caused, for example, by a massive ice sheet discharge) are quickly flushed out into the Pacific by the strong Southern winds (when the BS is open). Such a quick recovery is not possible in the closed BS case. For these cases of total NADW formation collapse we do not solve explicitly for the entire time-dependent overturning, but rather, deduce the systems response from the two end states (i.e., the arrested and resumed overturning).

Although the perturbations displayed in Fig. 1 are clearly large, we also derive a solution for the time-dependent response of the overturning to small perturbations (i.e., weak freshenings that cause small changes). We find that small perturbations are also removed quickly from the system but, in this limit, there is not much difference between the open and closed basin cases. We then proceed and examine analytically what kind of freshwater flux is required in order to collapse the MOC (Section 4) and what kind of continuous freshwater flux is required in order to maintain the collapsed state and prevent a recovery of the MOC. We find that, in order to collapse the MOC, about 0.19 Sv is required in both the closed and open BS case. However, in the closed basin case, even a zero freshwater flux will prevent the MOC from recovering. By contrast, in the open basin case, a continuous freshwater flux of 0.19 Sv is required in order to avoid recovery. This will again illustrate that the open BS is more stable than the closed BS. The above analytical analysis is followed by numerical experiments which confirm the results of the large perturbation analysis (Section 5). The results are summarized in Section 6.

2. The mean state model

Our (hybrid) model is a mixture of a global dynamical model and a box model representing the fraction of the NA situated between 50°N and 70°N. The transports into and out of the box are derived analytically from the momentum equations (for any salinity and temperature fields), but the bulk thermodynamic relations take the salinity and temperature to be fully mixed inside the box.

2.1. The dynamic model

Our analysis of the MOC in the Atlantic is based on an application of the "Thermodynamic Island Rule" (TIR) to the continents of the Americas in a similar fashion to (Nof, 2000). The TIR is an extension of the original Island Rule (Godfrey, 1989) which corresponds to an integration of the horizontal momentum equations along a closed path that avoids the frictional Western boundary current region (Fig. 2). The result is an expression of the circulation around the island in terms of the wind field along the path. The TIR differs from the original Island Rule in that sinking is allowed east of the island. Consequently, the circulation around the island is no longer a constant, but instead, the transport into and out of the basin (east of the island) differs by an amount equal to the sinking in

the basin east of the island. Furthermore, unlike the original Island Rule, we choose to integrate the momentum equations from the surface to a fixed depth, rather than to a level-of-no-motion. This allows us to choose any depth (above the topography) as the bottom of our upper layer, and, furthermore, with the steady state assumption it dispenses with the necessity to make the level-of-no-motion assumption (which is somewhat questionable in high latitudes).

(a) *TIR derivation*: The linearized Boussinesq momentum equations for a continuously stratified fluid, integrated from the surface to a fixed depth, H, below the Ekman layer (so that the stress is zero) and above the bottom topography are

$$-\rho_o fV = -\frac{\partial P}{\partial x} + \tau^x, \tag{1}$$

$$\rho_o fU = -\frac{\partial P}{\partial y} + \tau^y - RV, \tag{2}$$

where ρ_o is the mean density, f the coriolis parameter and U and V are the depth integrated zonal and meridional velocity, respectively. P is the depth integrated pressure (from the surface to H, a predetermined depth which is not necessarily a level-of-no-motion) and τ^x and τ^y are the surface wind stresses in the x and y directions. Note that, for clarity, all variables are defined in both the text and the appendix. Eqs. (1) and (2) correspond to a Sverdrup interior and frictional western boundary currents. Most of the energy dissipation occurs in the western boundary region through the term RV (where R is a frictional parameter).

We integrate (1) along AB and CD (Fig. 2) and (2) along BC and DA. Adding the four resulting equations eliminates the pressure and yields

$$\rho_0(-f_1 Q_1 - f_2 Q_2) = \oint \tau^r \, \mathrm{d}r, \tag{3}$$

where, the subscripts 1 and 2 refer to the southern and northern island tips so that Q_1 and Q_2 are the equatorwards transports across AB and CD, respectively. The integral $\oint \tau^r \, \mathrm{d}r$ is the counterclockwise integrated wind stress along the path. Because the frictional term RV is of the same order as the pressure term only in the western boundary region (which we avoid), it does not enter our calculation.

Next, we use mass conservation in the upper layer to close the problem

$$W = Q_1 + Q_2 + F_F, \tag{4}$$

where W is the water that sinks from the upper to the lower layer [O(10 Sv)], and F_F is the much smaller (known) freshwater flux [O(0.1 Sv)] which, though small, cannot always be neglected and needs to be carefully treated. (Note that this is where we digress from the original Island Rule, which assumes a level-of-no-motion as a vertical integration limit and takes $W = 0$.)

Solving for Q_1 and Q_2 in terms of W and F_F gives the two equations of the TIR,

$$Q_1 = \frac{\oint \tau^r \, \mathrm{d}r + \rho_0 \, f_2(W - F_F)}{\rho_0(f_2 - f_1)}, \tag{5}$$

$$Q_2 = -\frac{\oint \tau^r \, \mathrm{d}r + \rho_0 \, f_1(W - F_F)}{\rho_0(f_2 - f_1)}. \tag{6}$$

It should be emphasized that the level-of-no-motion assumption is not made here. It is merely required that the integration be done from the free surface to some level above the major topographical features (e.g., the mid-Atlantic ridge). It will become clear later that we do not consider the BS sill to be "major". Neglecting storage in the Arctic, we shall apply the TIR to the continents of the Americas in a similar fashion to Nof (2000) except that, here, we allow for a flow through the BS. We take not only the sea level to be continuous across the BS, but the entire vertically integrated pressure, P, is also taken to be continuous across the BS sill. The validity of this assumption is discussed in detail in Nof (2000, 2002) and need not be repeated here. It is sufficient to point out here that there is no physical process, such as a hydraulic control or frictional resistance, which would prevent the BS from allowing a much larger flow through it than it does today ($\sim$1 Sv). For instance, a speed of 1 ms^{-1}, which is not uncommon in straits, would correspond to a BS through flow of about 10 Sv.

(b) *The neglect of frictional and form drag in the BS*. In what follows we shall discuss the implications of the sea-level drop along the BS. First, it is important to realize that, with a barotropic geostrophic flow of 0.8 Sv (through the BS), a

depth of 50 m and a coriolis parameter of 1.4×10^{-4} s^{-1}, a 22 cm sea level difference between the Arctic and Pacific is induced. This sea level difference is due to geostrophy (i.e., it is obtained from $fQ = gH\Delta\eta$) and, hence, is across the flow rather than along it. As such, it is implicitly included in our calculations. Via geostrophy, zonal flows [of O(0.1) m s^{-1}] perpendicular to the axis of the strait (i.e., flows that do not cross from one basis to the other) can cause an additional sea level difference of perhaps 10 cm. Since the flows do not cross the boundary between the basins they are also not excluded from our calculation. Both of these sea level changes need to be distinguished from frictional and form-drag losses along a streamline which are neglected in our calculations.

One estimate for the frictional sea level drop can be obtained from the so-called Manning's formula, traditionally used by engineers to estimate the frictional pressure gradient in channels (Chow, 1959; Giles, 1962; Chaudry, 1993) but also used by geologists to estimate the flow from the paleo-Mediterranean to the (then freshwater lake) Black Sea. Taking a speed of 0.2 m s^{-1} (corresponding to a width of approximately 100 km), a frictional coefficient as large as can be reasonably expected ($n = 0.03$), and a length of 100 km, one obtains a negligible sea level drop of about 2 cm. Similar values are obtained by following the more traditional oceanographic estimates. To do so, we consider the familiar vertically integrated relationship

$$g\frac{\partial \eta}{\partial y} = \frac{1}{\rho_0}\frac{\partial \tau}{\partial z}$$

and take the bottom stress (divided by ρ_0) to be $C_D(u_*)^2$ where C_D (the dimensionless drag coefficient) is 1.6×10^{-3}, and u_* is the speed. With an along-strait distance of 100 km(Δy), and a mean speed u_* of 0.2 m s^{-1}, we again get a negligible drop ($\Delta\eta$) of merely 1 cm. Hence, the frictional forces are probably not important within the BS. Note that, in his pioneering freshwater analysis, Stigebrandt (1984) neglected the important effects of rotation and this forced him to choose parameters which would give him a frictional sea level drop of 50 cm. This 50 cm sea level drop is based on Reid's (1961) dynamics height analysis. While there is no doubt that there could indeed be a 50 cm difference between the Atlantic and the Pacific, this difference is not necessarily along a streamline and, consequently, is probably a representation of sea level differences due to geostrophy and density variations (calculated earlier) rather than due to frictional forces. Stigebrandt took a large value for the transport (1.6 Sv instead of 0.8 Sv), a large value for C_D (3×10^{-3} instead of 1.6×10^{-3}), and a much longer (200 km) and narrower (50 km) channel than ours (100×100 km). Stigebrandt himself realized that the neglect of rotation is not justified and that his calculation was somewhat questionable. Observations made after the publication of his work showed that his choices for the transport and width correspond to unrealistically high speed (four times higher than the observed values). Given that the frictional forces are proportional to the square of the velocity and that all his other choices were also on the high side, his selections were enough to push the frictional losses to much higher values.

A potentially problematic issue is the form-drag induced by the BS sill which is also not easy to estimate. Using our numerical simulations (5) we shall show that, even a sill protruding up to 50 m from the free surface (i.e., a sill blocking 93% of the upper layer), causes a deviation of no more than 40–50% from our sill-free calculations. This is because the flow through the strait is much smaller than the flow which the strait is capable of transporting. (As mentioned, a speed of 1–2 m s^{-1} which is common in many straits would lead to a transport of 10–20 Sv.) Overall, it can be stated that the assumption of a continuous vertically integrated pressure through the BS (i.e., neglecting the form-drag) is certainly adequate for the purpose of our calculation.

With the above neglect, integration of 40 years of NCEP annual winds[1] along the path shown in Fig. 2 gives 3.9 Sv for the first term in (5) and (6) [i.e., $\oint \tau^r \, dr/\rho(f_2 - f_1)$]. The coriolis parameters f_1 and f_2 were evaluated at 45°S and 75°N,

[1] NCEP winds were provided by the NOAA-CIRES Climate Diagnostics Center, Boulder, CO from their web site at http://www.cdc.noaa.gov.

respectively. (Note that, using an average coriolis parameter introduces an error of approximately 10%.) It is important to realize that this 3.9 Sv is the amount of water that will be forced out of the Atlantic and into the Pacific (via the BS) in the no NADW formation case (Fig. 2). Note that, in Nof (2000), Q_2 was taken to be zero and W was calculated from (6) according to the relationship

$$W = \frac{\oint \tau^r \, \mathrm{d}r}{\rho_0 f_1}.$$

This gave 9 Sv for both Q_1 and W which is about twice the no-NADW through flow calculated here [as should be the case because $f_1 \approx -(f_2 - f_1)/2.5$ so that (5) gives a Q_1 of about 4.0 Sv for $W = 0$].

2.2. The thermodynamics of the model

In the previous section, the transport into the Atlantic was derived in terms of the global wind field and the rate of NADW formation. We now assume that all the sinking occurs through deep convection between 50°N and 70°N so that Q_1 and Q_2 are also the transports into the box (shown in Figs. 2 and 3) from the south and the north, respectively. We shall now close the problem by relating the NADW formation rate to the NA surface salinity and expressing the NA salinity in terms of the incoming flows (Q_1 and Q_2).

The salinity in the convection region, S, is determined by the equation for the conservation of salt

$$M\frac{\partial S}{\partial t} = [(S_1 - S)Q_1 + (S_2 - S)Q_2 - SF_F], \tag{7}$$

where M is the volume of the region in which the sinking occurs (Fig. 2) and $S_{1,2}$ are the salinities of the incoming water Q_1 and Q_2. Both Qs are taken to be positive toward the Atlantic. The last term, SF_F/M, where F_F is the surface freshwater flux (precipitation minus evaporation plus runoff) into the region, represents a virtual salinity flux. For a steady state (4) and (7) give

$$WS = S_1Q_1 + S_2Q_2. \tag{8}$$

When Q_2 is negative, the equation needs to be altered because S_2, the salinity of Pacific water, is no longer relevant to the salinity in the Atlantic. Specifically for this case this steady state version of (7) takes the from, $Q_1(S_1 - S) = F_F S$. Note also that (8) needs to be modified for the cases where sea-ice is formed but we shall not deal with that situation.

In our model, NADW is formed by cooling the surface water until it reaches the density of the deep water. This is reflected in the steady conservation of heat relationship

$$0 = (T_1 - T)Q_1 + (T_2 - T)Q_2 + (T_a - T)F_F - \frac{F_H}{\rho C_p}, \tag{9}$$

where F_H is the surface heat flux for the box (in watts), ρ the reference density, C_p the heat capacity of sea water, T the temperature of the convective water, and T_1, T_2 and T_a are the temperatures of the incoming waters (Southern Ocean water, Pacific water and precipitation).

Next, we note that the temperature change brought about by the heat flux should be large enough to enable the upper water to reach the lower layer density. This convection condition is found from the linearized equation of state to be

$$T = T_l + \frac{\beta}{\alpha}(S - S_l), \tag{10}$$

where α and β are temperature and salinity expansion coefficients, and T_l and S_l are the temperature and salinity of the lower layer. It should be stressed that, in this model, the Southern Ocean (SO), the Pacific Ocean (PO), and the deep Atlantic are taken to be infinitely large so that their salinities and temperature are constants. This enables us to take S_1, S_2, T_1, T_2, S_l and T_l to be given.

2.3. The present mean circulation

The five algebraic equations (5), (6), (8)–(10) fully describe our system for the five unknowns Q_1, Q_2, W, S and T. To obtain the solution the heat flux equation (9) is rewritten as

$$WT - Q_1T_1 - Q_2T_2 - F_FT_a = -\frac{F_H}{\rho C_p}, \tag{11}$$

which, with the aid of the convection condition (10), can be written as

$$W\left[T_1+\frac{\beta}{\alpha}(S-S_1)\right]-Q_1T_1-Q_2T_2-F_FT_a=-\frac{F_H}{\rho C_p}. \quad (12)$$

Incorporation of the salinity conservation (8) into (12) gives a linear equation for W

$$W\left[T_1+\frac{\beta}{\alpha}S_1\right]+\frac{\beta}{\alpha}(S_1Q_1+S_2Q_2)-Q_1T_1-Q_2T_2-F_FT_a=-\frac{F_H}{\rho C_p}. \quad (13)$$

where Q_1 and Q_2 are also linear in W and are given by (5) and (6). Since $F_F \ll Q_{1,2}$ [i.e., $F_F \sim O(0.1)$ Sv whereas $Q_{1,2} \sim O(1)$ Sv] the last term on the left-hand side of (13) can be neglected. Note that, unless otherwise stated, the freshwater flux in only neglected in the heat equation.

Our chosen modern-day parameters are: $f_1 = -1.0\times10^{-4}$ s^{-1}, $f_2 = 1.4\times10^{-4}$ s^{-1}, $M = 4\times10^{15}$ m^3 (corresponding to an area of 4000×1000 km^2 and a depth of 1 km), $F_H = 1.6\times10^{14}$ W (corresponding to COADS data of 40 W m^{-2}), $F_F = 0.15\times10^6$ m^3 s^{-1} (Schmitt et al., 1989), $\rho = 1000$ kg m^{-3}, $C_p = 4000$ J kg$^{-1}K^{-1}$, $\beta = 8\times10^{-4}$ PSU^{-1}, $\alpha = 1.5\times10^{-4}$ K^{-1}, $S_1 = 35.9$ PSU, $S_2 = 34.8$ PSU, $S_l = 34.9$ PSU, $T_1 = 10^\circ$C, $T_2 = 3^\circ$C, $T_l = 3.5^\circ$C. All were carefully determined from Tomczak and Godfrey (1994), the Levitus data and Gill (1982). (Note that T_2 and S_2 are taken as Arctic rather than Pacific values.) For these choices, the solution for the sinking is $W = 11.2$ Sv so that $Q_1 = 10.3$ Sv, $Q_2 = 0.8$ Sv, $S = 35.3$ PSU, and $T = 5.9^\circ$C.

For a closed BS, we take $Q_2 = 0$ and $W = Q_1 + F_F$; Eqs. (5) and (6) are now meaningless and we are left with three relations (8)–(10) for the three unknowns, Q_1, S and T. If we use the same numerical values as for the modern-day open BS case, we get $Q_1 = 10.4$ Sv, $S = 35.4$ PSU and $T = 6.1^\circ$C which are not that different from the open BS values. However, during glacial times, the parameters had different values and according to Romanova et al. (2004), Schäfer-Neth and Paul (2000) and Adkins et al. (2002), it is more appropriate to take a heat flux of 38 W m^{-2}, $F_F = 0.05$ Sv, $\alpha = 5\times10^{-5}$ K^{-1}, $S_l = 36.1$ PSU, $S_1 = 36.4$ PSU, $T_l = -1.2^\circ$C, and $T_1 = 5^\circ$C. For these values we get $Q_1 = 6.5$ Sv, $S = 36.1$ PSU, and $T = -0.9^\circ$C. It is important to realize that the glacial values rely on proxies and, therefore, should be interpreted with caution. The salinity estimates are of particular concern because of their role in the NADW formation process.

All of these chosen and calculated mean state values will shortly be used to calculate both the system's recovery time and the freshwater fluxes required for the arrest of the MOC.

3. Perturbations to the mean state

3.1. Large perturbations

Consider a very large freshwater anomaly that is sufficient to shut down the NADW formation completely.

(i) *Open BS*: We see from (5) and (6) that, when the BS is open and there is no NADW formation (i.e., $W = 0$), the strong winds in the SO would push about 4 Sv into the SA and then out of the NA, through the Arctic, and into the Pacific. This implies that such a NADW shut-off causes a reversal of the flow through the BS, i.e., instead of the presently known flow into the Atlantic, the flow would exit the Atlantic. We shall see in Section 5 that the sill in the BS could reduce the reversed flow by up to 50% (which means that there may be 2–3 Sv or so forced from the Atlantic into the Pacific instead of our calculated 4 Sv) but the remaining flux is still a significant amount. Hence, any salinity anomalies in the NA which are strong enough to collapse the MOC would be quickly flushed (laterally) out of the Atlantic via the open BS so that the MOC will rapidly recover (Fig. 1). It is important to realize that, in this stage, the box model does not have to be introduced yet and we can envision a salinity anomaly cap 50 m thick covering an area of 4000×1000 km^2. Removal of such an anomaly through a 4 Sv advection would take approximately 1 year.

(ii) *Closed BS*: When the BS is closed, the anomalies are trapped in the Atlantic and cannot

be flushed out. The MOC can still recover (Birchfield et al., 1994; Wang and Mysak, 2001; Ganopolski and Rahmstorf, 2001, 2002; Schmittner et al., 2002), but much more slowly than in the open BS case because the freshwater anomalies can no longer be horizontally advected out of the convection region. Two possible mechanisms for the removal of the freshwater anomaly (when the strait is closed) are diffusion and evaporation. For the open ocean away from topography and boundaries, the typical vertical eddy diffusivity is $0.1–10^{-4}$ m s^{-1} (Ledwell et al., 1993) which, with an anomaly thickness scale of 50 m, gives a diffusive time scale of 10 years. The evaporative time scale for a freshwater cap of 50 m thickness (corresponding to the break up of five ice sheets of $70 \times 70 \times 0.5$ km^3 a year during a period of 10 consecutive years which is analogous to pouring 0.2 Sv of freshwater for a period of 10 years) and an evaporation rate of 1 mm day^{-1} is $\sim$140 years. The evaporative estimate is based on "typical" freshwater with a salt constant of approximately 0.5 PSU. Converting this freshwater into salty oceanic water requires and evaporation of 98.5% of the water, implying that most of the freshwater cap was to be evaporated. These recoveries can, of course, be faster as the anomalies can certainly be shallower.

Sea ice which, through brine rejection, increases the salinity, also appears to be important (Paul and Schulz, 2002). However, the salinity increase is not strong enough to cause a recovery of a collapsed MOC as even the formation of 2 m of sea ice on top of a thermocline 500 m deep will increase the surface salinity by merely 0.14 PSU. This is much smaller than the typical difference between the upper and lower layer salinity in the Atlantic (1 PSU). Another negative feedback is due to local winds (Schiller et al., 1997). A collapsed MOC causes strengthening of the local winds (due to an enhanced equator–pole temperature gradient) which causes an increased local upwelling. This increases the surface salinity reducing the density difference (which the cooling needs to overcome). Taking an upwelling of 3 Sv and an upper water volume (of the northern NA) to be about 107 km^3, we find that it would take 100 years or so to replace it by deep water. This also implies a long recovery time.

Another mechanism by which the collapsed MOC can recover in the closed BS case is related to the atmospheric response to a shutdown (see e.g., Saravanan and McWilliams, 1995). In that case the atmospheric temperatures around the high latitude NA cools significantly following a thermohaline shutdown. The associated increase in heat loss can help to re-establish the overturning circulation within about 100 years. All these mechanisms point to a recovery time of hundreds of years which is considerably longer than the advection time in the open BS case.

3.2. Small perturbations

Although the perturbations prior to 12,000 years ago (illustrated by Fig. 1) do not appear to be small, it is useful to also examine the stability to small perturbations. Here, the perturbations to the system are regarded as small deviations from a mean state and we solve for the system's time-dependent response using the hybrid box model introduced earlier. As before, we shall consider the open and closed BS separately.

(i) *Open BS*: We shall perturb Q_1, Q_2, W, T and S. As before, since the SO, the PO and the deep Atlantic are all taken to be infinitely large, all the other variables are taken to be constant external parameters which do not react to the internal changes in the NA circulation. We now perturb the five equations around a mean state assuming that the time-dependent part of the terms in the island rule equations are small and negligible. This is based on the idea that the box has a fixed volume and that, in our model, there is no other light water storage in the Atlantic. Under such conditions the perturbed equations are

$$Q_1' = \frac{f_2 W'}{f_2 - f_1}, \tag{14}$$

$$Q_2' = -\frac{f_1 W'}{f_2 - f_1}, \tag{15}$$

$$M\frac{\partial S'}{\partial t} = (S_1 - \bar{S})Q_1' + (S_2 - \bar{S})Q_2' - S'[\bar{Q}_1 + \bar{Q}_2 + \overline{F_F}], \tag{16}$$

$$M\frac{\partial T'}{\partial t} = (T_1 - \bar{T})Q_1' + (T_2 - \bar{T})Q_2' - T'[\bar{Q}_1 + \bar{Q}_2 + \overline{F_F}], \quad (17)$$

$$T' = \frac{\beta}{\alpha}S', \quad (18)$$

where the primed variables are time dependent and the bar denotes the mean state.

Substitution of (18) into (17), subtracting the equation thus obtained from (16) and the incorporation of (14) and (15) shows that $Q_1' = Q_2' = W' = 0$ and that the solutions for S' and T' are decaying exponentials

$$S' = S_0\,\mathrm{e}^{-(\bar{W}/M)t}; \quad T' = T_0\,\mathrm{e}^{-(\bar{W}/M)t}, \quad (19)$$

showing that the small perturbation recovery time is approximately 11 years.

The stability is due to the wind-induced mean flows which, after a perturbation in the NA surface salinity, attempt to re-establish the mean state salinity. For example, after a freshening of the NA, the salinity of the incoming flows are constant, but the sinking water is now fresher. The salinity anomaly is, therefore, expelled out of the upper layer by the sinking of fresher (and colder) water. This means that, in contrast to the large perturbations (i.e., a complete NADW collapse) case when the salinity anomalies are flushed out laterally, the anomalies in the small perturbation case are flushed out vertically. This is done via the convection itself which is still active and pulls down the weak anomaly, pushing it into the infinitely large deep ocean.

(ii) *Closed BS*: When the strait is closed (14) and (15) are no longer valid. In this case, the system can still remove salinity perturbations via vertical flushing through the convection itself which again pulls the salinity disturbance down, pushing it into the deep ocean. Taking $Q_2 = 0$ and $W = Q_1 + F_F$, the earlier system of equations reduces to three equations with three unknowns (Q_1, S and T),

$$M\frac{\partial S}{\partial t} = (S_1 - S)Q_1 - SF_F,$$

$$M\frac{\partial T}{\partial t} = (T_1 - T)Q_1 + (T_a - T)F_F - \frac{F_H}{\rho C_p}$$

and Eq. (18). A perturbation analysis again shows that $W' = Q_1' = 0$ and that

$$S' = S_0\,\mathrm{e}^{-(\bar{W}/M)t}; \quad T' = T_0\,\mathrm{e}^{-(\bar{W}/M)t}.$$

For modern-day conditions, the recovery time (12 years) is approximately the same as that of the open case (about 11 years). For the glacial conditions mentioned earlier in Section 2.3, the recovery time is about 19 years, somewhat longer than in the open BS case.

All of this illustrates that, in the small perturbation case, there is no significant difference between the closed and open BS cases. This completes our formal small amplitude stability analysis and we shall now proceed to examine the critical freshwater fluxes which can arrest the MOC. We shall see that, in these important aspects, there is again a large difference between the open and closed cases.

4. Critical freshwater fluxes

The system of five steady equations (5),(6), (8)–(10) also allows for a detailed examination of the freshwater flux required for an MOC collapse. As mentioned, this is a more important issue than the small amplitude instability issue discussed earlier because the perturbations during glacial times (Fig. 1) do not appear to be small. There are three different critical freshwater fluxes. The reader is warned here in advance that the differences between these fluxes are quite subtle. The first (F_{Fa}) is the freshwater flux which makes the upper layer so light that the cooling is insufficient to cause convection. (Note that by "first" we merely mean the first freshwater flux that we shall deal with and not necessarily the smallest. It is, in fact, the largest of the three.) In this case, the wind removes the upper layer from the convection area so quickly that the cooling has no time to cause deep water formation. As we shall see, such an upper layer removal is only possible in the open BS case because, in the closed basin case, there is no process that can remove the water away from the cooling area, implying that any cooling will ultimately cause convection. We shall see that, for the modern-day parameters chosen earlier, the open BS critical freshwater flux turns out to be

about 0.2 Sv. This amount is about 0.05 Sv greater than the presently estimated flux of 0.15 Sv. This difference is equivalent to about half the mean discharge of the Amazon.

The second critical freshwater flux (F_{Fb}) is the near-freezing convective flux, i.e., the freshwater flux that makes the convective layer so fresh that the required cooling brings the sinking water to the freezing point. This situation is possible only in the closed BS because, in the open ocean case, the condition of no-convection due to wind action is reached prior to the freezing condition. We shall see that, for modern conditions, the closed BS case corresponds to a critical flux of 0.19 Sv.

The third freshwater flux (F_{Fc}) is the flux required to maintain the MOC in a collapsed state. We shall see that, here, there is again a large difference between the open and closed BS case. In the open BS, 0.20 Sv is required to maintain the collapsed state whereas in the closed BS case no amount of freshwater is needed to maintain the collapsed state. This is because our closed system cannot quickly recover from a collapse. This difference between the open and closed cases demonstrates again that the open BS case is much more resistant to perturbations than the closed BS case.

4.1. The first critical freshwater flux

(i) *Open BS*: To obtain this critical freshwater flux, F_{Fa}, we set $W = 0$ in Eqs. (5), (6) and (8). We also note that, here, $S_2 = S$ and $T_2 = T$ (because now the flow through the BS exits the Atlantic rather than entering it). This gives expressions for Q_1 and Q_2 in terms of F_{Fa},

$$Q_1 = \frac{\oint \tau^r \, \mathrm{d}r - \rho_0 \, f_2 F_{Fa}}{\rho_0 \, (f_2 - f_1)},$$

$$Q_2 = -\frac{\oint \tau^r \, \mathrm{d}r - \rho_0 \, f_1 F_{Fa}}{\rho_0 (f_2 - f_1)}$$

and

$$S_1 Q_1 = -S Q_2.$$

Elimination of Q_1 and Q_2 gives immediately an expression for F_{Fa} in terms of S,

$$F_{Fa} = \frac{(S_1 - S) \oint \tau^r \, \mathrm{d}r}{S \rho_0 (f_2 - f_1)}, \tag{20}$$

where the condition $\Delta S \ll S$ (so that $S_1 \approx S$) has been used (merely for simplicity). This together with the heat Eq. (9) and the island rule with the freshwater flux ignored (because $F_F \ll Q$), and the convection condition (10) gives

$$S = S_1 - \frac{\alpha}{\beta}(T_1 - T_1) - \frac{\alpha}{\beta} \frac{F_H (f_2 - f_1)}{C_p \oint \tau^r \, \mathrm{d}r}. \tag{21}$$

Substitution of the modern-day parameters chosen earlier into the heat equation (9) again with the freshwater flux ignored gives $T = -0.02^\circ$C right away. The salinity is found to be 34.24 PSU [either from the convection condition (10) or from (21)]. Recalling that the no-W island rule calculation gives 4 Sv [i.e., $\int \tau^r \, \mathrm{d}r/(\rho_0(f_2 - f_1)) = 4$ Sv] and using (20) shows that $F_{Fa} = 0.19$ Sv. Because of the low temperature, it is perhaps more appropriate here to use a lower value of α. Taking α to be half of the commonly used value we find the temperature is unaltered ($T = -0.02^\circ$C) but the salinity slightly increases to 34.46 PSU and F_{Fa} slightly decreases to 0.17 Sv.

(ii) *Closed BS*: In the closed BS case ($W = Q_1; Q_2 = 0$), there is no steady solution for $W = 0$ because the upper water cannot be removed from the convection area. Consequently, even with a small amount of cooling, the water ultimately sinks.

4.2. The second critical freshwater flux

(i) *Open BS*: In contrast to the earlier case where we set W to zero, we now obtain the near-freezing collapse by leaving W free and adding the (approximate) freezing condition,

$$T = -\delta S, \tag{22}$$

where the density tables give an approximate value for δ of $0.0575^\circ K/\mathrm{PSU}$. With (22) and Eqs. (5), (6), (8)–(10) we can now solve for the six unknowns W, Q_1, Q_2, S, T and F_{Fb}. Eqs. (22) and (10) immediately give the solution for T and S,

$$T = \frac{-\delta S_1 \beta/\alpha + \delta T_1}{\delta + \beta/\alpha}, \tag{23}$$

$$S = \frac{S_1\beta/\alpha + T_1}{\delta + \beta/\alpha}, \tag{24}$$

which, for our chosen modern-day parameters give $T = -1.95^\circ$C and $S = 33.9$ PSU.

Elimination of Q_1 between (3), which is just a combination of (5) and (6), and (9) gives,

$$Q_2 = \left[-\frac{f_1 F_H}{\rho_0 C_p} + \frac{T - T_1}{\rho_o}\oint \tau^r \, dr\right] / [f_1(T - T_2) - f_2(T - T_1)]. \tag{25}$$

The critical freshwater flux can now be found to be

$$F_{Fb} = \left[-\frac{\oint \tau^r \, dr}{f_1\rho_0} - \frac{f_2 Q_2}{f_1}\right]\left(\frac{S_1}{S} - 1\right) + Q_2\left(\frac{S_2}{S} - 1\right) \tag{26}$$

and, as before, (4) and (8) combine to give

$$Q_1 = \frac{FS + Q_2(S - S_2)}{S_1 - S}. \tag{27}$$

As expected, for the modern-day values mentioned earlier, one finds from (4), (8), (25) and (26), that the MOC collapse due to the strong southern winds (which push the water away from the convection region) occurs before the water can freeze. This implies that the freezing condition is irrelevant to the open Atlantic and, consequently, the corresponding values are not given here. We shall see shortly that this is not the case for the closed BS where freezing is the only mechanism which can terminate the convection (in our model).

(ii) *Closed BS*: In the closed BS case, (10) and (22) still hold but (5) and(6) are no longer relevant and (8) and (9) become

$$(Q_1 + F_F)S = Q_1 S_1, \tag{28}$$

$$Q_1(T - T_1) = -F_h/(\rho_o C_p), \tag{29}$$

from which Q_1 and F_{Fb} can be easily computed. Note that, as before, the freshwater term was neglected in the heat equation (because $F_F \ll Q$) and that the earlier computed freezing condition values for S and T are still relevant. For the modern-day parameters chosen earlier, we now find that $Q_1 = 3.35$ Sv and $F_{Fb} = 0.20$ Sv, showing that for this kind of collapse there is no real difference between the closed and open cases.

4.3. Maintaining a collapsed MOC state

Here, we ask the question of what will it take to keep the MOC in a collapsed state. For the chosen modern-day parameters, the open BS collapse–maintenance freshwater flux is identical to the collapsing flux of 0.19 Sv. This is not the case, however, with the closed BS case. Our closed case model cannot (quickly) recover from a collapse implying that a *zero* freshwater flux is required for the maintenance of a closed-basin collapsed state. Since the open BS requires a significant freshwater flux (0.19 Sv) to maintain its collapsed state we again see that it is much more stable than the closed case. This completes our study of the analytical model. We shall now proceed to a numerical examination of the problem.

5. Numerical simulation

Instead of verifying our analysis using very complicated numerical models (corresponding to Fig. 2), the application of (5) and (6) to the model shown in Fig. 4 (which does not contain meridional winds) was examined. To do so, a "reduced gravity" version of the Bleck and Boudra isopycnic model (Bleck and Boudra, 1981, 1986; Bleck and Smith, 1990) was used. Namely, we took the upper layer density to be constant in our numerical simulations. A continuously stratified upper layer with variable density would have been better, but, since the ocean will always adjust its temperature and salinity field (according to the buoyancy exchange with the atmosphere) so that (5) and (6) are satisfied, this is not an issue. Recall that in the analytics Q_1 and Q_2 were specified and the NADW formation rate W was calculated as part of the problem. By contrast, in the numerics, W must be specified and Q_1 and Q_2 adjust accordingly.

We performed two sets of experiments totaling 16 experiments. Out of the 16 experiments, 8 were without NADW, i.e., they corresponded to a collapsed MOC state. To examine the relationship between the numerical model and the analytical theory, experiments were performed where the wind stress (Fig. 4) was varied with a fixed gap (exp. 1–8).

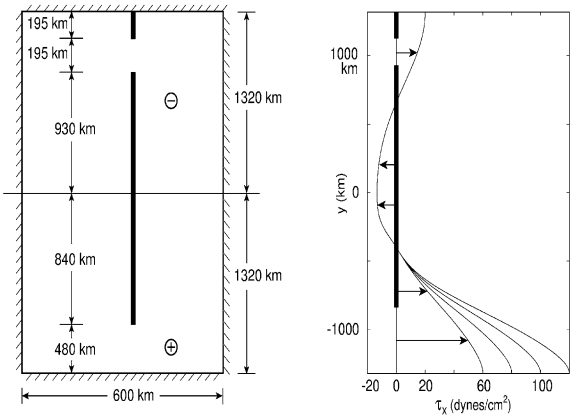

Fig. 4. (Left panel) Details of the basin used for the two sets of numerical experiments. The source and the sink $\oplus$, $\ominus$ were only used in the second set which involved NADW. Note that the Bering Strait contains a sill. In all the experiments $\Delta x = \Delta y = 15$ km, $\Delta T = 360$ s. (Right panel) The amplified wind profile used for the simulations. Note that the amplification has two components. The basic amplification was adopted due to the magnified β and reduced basin width both of which were adopted to make the runs more economical. The second amplification indicates the ratio between the winds along the southern boundary and the winds along the northern boundary. It ranges from 3 to 6 and represent various southern winds. The general profile was adapted from Hellerman and Rosenstein (1983).

To examine how NADW formation affects the transports, we also performed experiments with a sink in the North Atlantic (exp. 9–16) whose flux W was specified. To verify that the presence of a sill across the Bering Strait is not important, we repeated the varying wind and upper water removal experiments with a sill extending all the way from the bottom to 50 m from the free surface (blocking 93% of the total undisturbed depth of 600 m). This sill corresponds to the situation associated with the Bering Strait. We shall see that the results of the sill and no-sill experiments were similar but the sill clearly retards the flow.

The sill was implemented by keeping the upper layer depth fixed (at, say, 50 m) within the gap itself and leaving the depth east and west of the gap free. Hence, the presence of the sill enters the momentum equations directly only through the lateral friction terms. (Indirectly, it enters through the speeds and pressure.) Similarly, it directly enters the continuity equation by restricting the volume flux through the gap. (Note that the velocity and pressure adjust each other across the gap.) To represent the overturning, a (mass flux) source at the center of the southern boundary and a sink in the northern basin were introduced.

As in Nof (2000, 2002), to make our runs more economical we used a magnified β^*, a magnified wind stress τ, and a reduced basin size. We chose β^*, the linear variation of the coriolis parameter with latitude, to be 11.5×10^{11} m^{-1} s^{-1}, g the reduced gravity to be relatively large 0.15 m^2 s^{-1} (again to speed up the calculation), h the undisturbed thickness to be 600 m, ν the eddy viscosity to be 2000 m^2 s^{-1}, K the linear drag to be 20×10^{-7} s^{-1}, $\Delta x = \Delta y = 15$ km, and $\Delta t = 360$ s. The flushing of a hypothetical salinity anomaly is shown in Fig. 5. Fig. 6 shows the numerical transports and their relationship to the analytics for the varying wind experiment. There is a good agreement of the nonlinear numerical simulations and the no-sill analytical computation no matter how strong the wind is. The effect of a sill displays a fair (but not good) agreement of the analytics with the numerics. As expected, the discrepancy is greatest when the sill protrudes almost all the way to the surface. Given that the sill blocks 93% of the upper layer thickness, the effect of the sill is relatively small. This is because the modeled BS transport is much smaller than the amount that the strait is capable of handling. (It is mentioned here in passing that this is also the situation in nature.)

As is typical for this sort of island calculation, which (among other things) neglect zonal boundary currents, it is not a simple matter to explain the details of the numerics. This was pointed out in Nof (2000, 2002) where an attempt was made to explain the relationship between the slope of the curves describing the numerics and the analytics. It is also not clear why the numerical Q_2 is greater than the analytical for the no-NADW case and yet smaller than the analytical for the case with NADW formation.

6. Discussion and summary

The opening of the BS is proposed as an explanation for the marked difference between

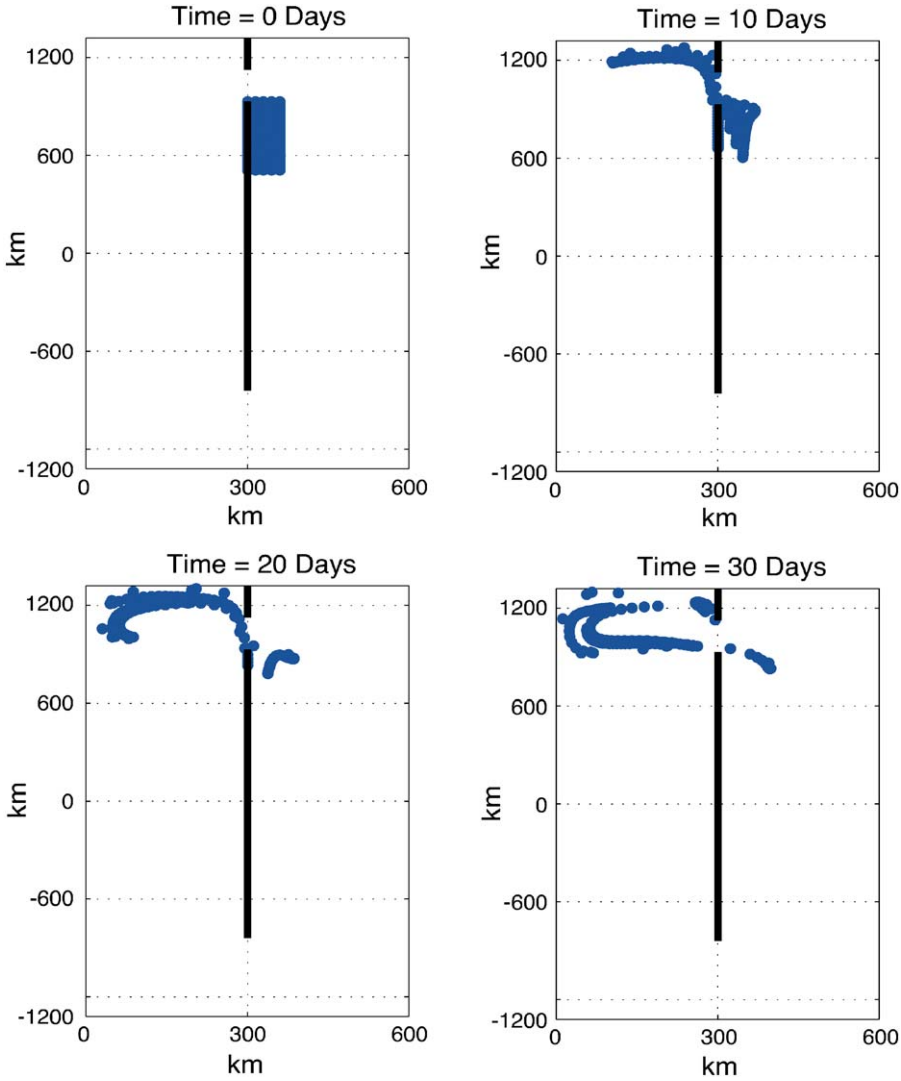

Fig. 5. "Reduced gravity" numerical experiment (exp. 5) showing how a hypothetical freshwater anomaly which is strong enough to shut the NADW off is flushed out of the Atlantic within a short time. The upper layer has one density and the anomaly is represented by dyed fluid. It is 80×50 km in size and occupies the entire upper layer thickness (with no density anomaly).

the stability of the glacial and interglacial climate (Fig. 1). We focused on the case of a large perturbation, i.e., a massive ice sheet discharge or other freshwater source which shuts down the NADW formation completely.

This example of a fully arrested overturning (caused by a large freshwater anomaly in the NA such as an Heinrich event) illustrates the importance of the strong SO winds and the open gateway of the BS during interglacials to the thermohaline stability. The Island Rule states that, under such conditions, the SO winds would push $\sim$4 Sv into the Atlantic (Fig. 2). This 4 Sv would then flow straight through the NA and into the Pacific via the BS, taking with it the freshwater anomaly causing the disruption. These results were verified using a process oriented numerical model (Figs. 5 and 6). Once the NA regains its former

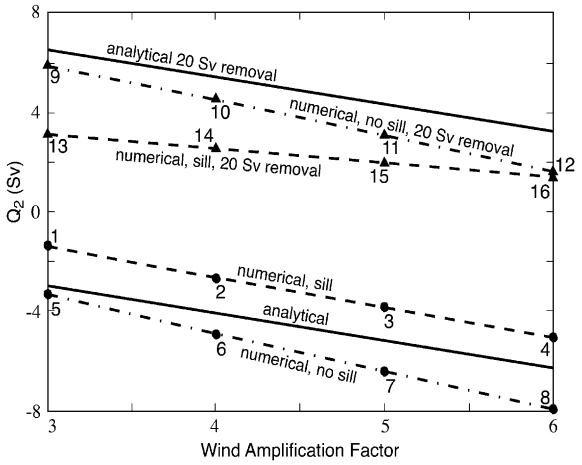

Fig. 6. The 16 numerical experiments and their relationship to the analytics (solid lines). The first set (exp. 1–8) does not involve NADW whereas the second (exp. 9–16) involves 20 Sv of NADW (which was artificially introduced to the system through the source and the sink). As expected, the experiments with a sill (protruding up to 50 m from the free surface implying a 93% cross-sectional blockage) show a smaller transport than both the sill-free experiments and the analytics. The difference, however, is not so great because, even with the sill, the strait can accommodate a much larger volume flux than it actually does. Numerals indicate experiment number.

salinity, the overturning is quickly (within several years) re-established. In the closed BS case, the freshwater anomaly is prevented from escaping through the strait. It may be removed by diffusion or eliminated by either evaporation or enhanced atmospheric cooling but all of these processes take much longer, about 50–1000 years.

An analytical model combining the gigantic island calculations with a box model enables us to compute the critical freshwater fluxes required to collapse the MOC in both the open and the closed cases. We find that, in the open BS case, a freshwater flux of 0.19 Sv is required to collapse the cell and maintain the collapsed state. Namely, in the open BS case, a recovery quickly occurs unless 0.19 Sv is *continuously* dumped into the open NA. In contrast, in the modern closed BS case, 0.20 Sv is sufficient to collapse the cell but *no* freshwater flux is required to maintain the collapsed state. That is, in the modeled closed case, the MOC does not recover even when the freshwater flux is reduced to zero. This again shows that the modeled open BS is much more stable than the modeled closed BS case.

Although the glacial perturbations displayed in Fig. 1 are large, a small perturbations analysis around a mean state was also performed. As before, the hybrid-dynamical-box model includes not only the effect of the thermodynamic surface forcings to the thermohaline circulation, but also the important effect of the global winds and the meridional flow that they induce. We found that small perturbations to the temperature and salinity would be damped out with a rapid e-folding scale of 11 years. The damping takes place because the convection is still active so that it pulls the salinity anomaly down to the deep ocean. Namely, in contrast to the large perturbation case where the anomaly removal is due to a *lateral* flushing, the removal here is due to *vertical* flushing. In the closed basin case, weak perturbations can also recover through vertical flushing by the convection itself. For modern-day conditions, the time scale for this process is about 12 years—a bit slower than in the open BS. For glacial conditions the closed NA recovery time is somewhat longer, about 26 years. It is important to realize that the absence of a large perturbation from the interglacial record shown in Fig. 1 does not at all mean that there were no large perturbations during that period. The absence may merely mean that they were wiped out very quickly.

The simplicity of the model naturally brings along a couple of weaknesses which need to be mentioned. First, the complex dynamics of localized convection is not accurately resolved in our large box domain and our simple conditions for convection. We simply captured the connection between the NADW formation to the NA surface salinity using some basic physical principles. Second, changes in the salinity of the box was determined in the classical box model style, i.e., by taking a pure salinity mix of the net incoming and outgoing flows and accounting for the surface boundary conditions (Stommel, 1961; Park, 1999; Marotzke, 2000). The method neglects other mixing process such as flows into and out of the box that have no net transport (e.g., horizontal gyres).

Another alternative explanation for the difference in glacial and interglacial climate stability

might be that there simply were no ice sheets that would break after the BS opened. We reject this explanation on the ground that large ice sheet discharges are not the only means of perturbing the thermohaline circulation (Peterson et al., 2000; Ganopolski and Rahmstorf, 2002; Rahmstorf and Alley, 2002) and on the ground that this transition also could not have happened abruptly. We argue that the opening of the BS could have occurred abruptly due to an initial jamming of the strait by icebergs and broken ice sheets which congregated around the BS because of the funnel-like shape of the surrounding continent. This jamming continued until the size of the icebergs was reduced to a size that could pass through the strait and the sea level difference between the Arctic and Pacific was large enough to break the 'dam'.

It should be stressed that, like all model studies, our results are somewhat speculative. The results of both simplified models such as ours (which neglect many ocean processes) and complicated climate models (which unavoidably use very high vertical diffusivities) should be interpreted with much caution. Surely, analytical models have their limitations but so do complicated climate models. Relatively complex climate models suffer from the familiar weakness that all general circulation models suffer from—the results of simulations involving convection of roughly 10–20 Sv are very sensitive to the specified vertical eddy diffusivities (roughly 0.5 $cm^2\ s^{-1}$) which are typically an order of magnitude higher than the observed values (0.1 $cm^2\ s^{-1}$).

This is not a trivial matter considering that the commonly used numerical diffusivity of 0.5 $cm^2\ s^{-1}$ is associated with a conversion of as much as 10 Sv of upper ocean water to lower layer water or vice versa. (This scaling estimate is based on a thermocline 500 m deep and an Atlantic surface area of $5000\ km \times 20,000\ km$.) It is particularly troublesome for simulations involving flows through straits and passages because the transport in many passages is of the order of one Sverdrup, much smaller than the diffusion-induced transport. As a result, several numerical simulations predict flows (through straits) which are not even in the same direction as the observations (Nof and Van Gorder, 2003).

Consequently, it is best to examine the natural phenomenon in question using different techniques and approaches with the hope that all of them can be ultimately combined into a more reliable and comprehensive picture of the system.

Acknowledgements

This study was supported by the National Aeronautics and Space Administration under Grants NAG5-7630 and NGT5-30164; National Science Foundation Contract OCE 9911324 and OCE-0241036; and Office of Naval Research Grant N00014-01-0291.

Appendix A

A.1. List of symbols

α	temperature expansion coefficient
β	salinity expansion coefficient
β^*	linear variation of the Coriolis parameter with latitude
C_D	dimensionless drag coefficient
C_p	heat capacity of sea water
f	coriolis parameter
$f_{1,2}$	coriolis parameters along the southern and northern island tips (Fig. 2)
F_F	freshwater flux into convection region (Fig. 3)
$F_{Fa,Fb,Fc}$	first and second and third critical freshwater fluxes
F_H	heat flux out of convection region (Fig. 3)
g	gravitational constant
h	upper layer depth of numerical model
H	upper layer depth of analytical model
K	linear drag coefficient of numerical model
M	volume of the convection region
η	sea level height anomaly
P	vertically integrated pressure
Q_1, Q_2	southern and northern transports into the island basin (Figs. 2 and 3)
ρ	mean density of water in the convection region

ρ_0	mean ocean water density
r	integration path
R	interfacial friction coefficient
S	salinity of the water in the convection region
S_1, S_2	salinities associated with the transports Q_1, Q_2
S_l	salinity of the lower layer
U, V	vertically integrated velocities in the x and y directions
W	net sink of water from the upper to the lower layer
τ^r	wind stress in the direction r
T	temperature of the water in the convection region
T_1, T_2	temperatures associated with the transports Q_1, Q_2
T_l	temperature of the lower layer
T_a	atmospheric surface temperature over convection region
v	eddy viscosity of numerical model

References

Adkins, J.F., Boyle, E.A., Keigwin, L., Cortijo, E., 1997. Variability of the North Atlantic thermohaline circulation during the last interglacial. Nature 390, 154–156.

Adkins, J.F., McIntyre, K., Schrag, D.P., 2002. The salinity, temperature, and δ^{18}O of the glacial deepn ocean. Science 298, 1769–1773.

Bard, E., 2002. Climate shock: abrupt changes over millennial time scales. Physics Today 55, 32–38.

Bard, E., Rostek, F., Turon, J.-L., Gendreau, S., 2000. Hydrological impact of Heinrich events in the subtropical northeast Atlantic. Science 289, 1321–1324.

Birchfield, E.G., Wang, H., Rich, J.J., 1994. Century/millennium internal climate oscillations in a ocean–atmosphere–continental ice sheet model. Journal of Geophysical Research 99 (C6), 12459–12470.

Bleck, R., Boudra, D., 1981. Initial testing of a numerical ocean circulation model using a hybrid, quasi-isopycnic vertical coordinate. Journal of Physical Oceanography 11, 755–770.

Bleck, R., Boudra, D., 1986. Wind-driven spin-up in eddy-resolving ocean models formulated in isopycnic and isobaric coordinates. Journal of Geophysical Research 91, 7611–7621.

Bleck, R., Smith, L.T., 1990. A wind-driven isopycnic coordinate model of the North and Equatorial Atlantic Ocean, 1, Model development and supporting experiments. Journal of Geophysical Research 95, 3273–3285.

Blunier, T., Chappelaz, J., Schwander, J., Dallenbach, A., Stauffer, B., Stocker, T.F., Raynaud, D., Jouzel, J., Clausen, H.B., Hammer, C.U., 1998. Asynchrony of Antarctic and Greenland climate change during the last glacial period. Nature 394, 739–743.

Bond, G., Broecker, W., Johnson, S., McManus, J., Labeyrie, L., Jouzel, J., Bonani, G., 1993. Correlations between climate records from North Atlantic sediments and Greenland ice. Nature 365, 143–147.

Boyle, E.A., 2000. Is the ocean thermohaline circulation linked to abrupt stadial/interstadial transitions. Quaternary Science Reviews 19, 255–272.

Broecker, W.S., 1994. Massive iceberg discharges as triggers for global climate change. Nature 372, 421–424.

Cacho, I., Grimalt, J.O., Pelejero, C., Canals, M., Sierro, F.J., Flores, J.A., Shackleton, N., 1999. Dansgaard–oeschger and Heinrich event imprints in Alboran Sea paleotemperatures. Paleoceanography 14 (6), 698–705.

Chappell, J., Shackleton, N.J., 1986. Oxygen isotopes and sea level. Nature 6, 183–190.

Chappell, J., Omura, A., Ezat, T., McCulloch, M., Pandofi, J., Ota, Y., Pillans, B., 1996. Reconciliation of late quaternary sea levels derived from coral terraces at Huon Peninsula with deep oxygen isotope records. Earth and Planetary Science Letters 141, 227–236.

Chaudry, M.H., 1993. Open Channel Flow. Prentice-Hall, Inc., Englewood Cliffs, NJ, 483pp.

Chow, V.T., 1959. Open-Channel Hydraulics. McGraw-Hill, New York, 680pp.

Clark, P.U., Pisias, N.G., Stocker, T.F., Weaver, A.J., 2002. The role of the thermohaline circulation in abrupt climate change. Nature 415, 863–869.

Dansgaard, W., Johnsen, S.J., Clausen, H.B., Dahl-Jensen, D., Gundestrup, N.S., Hammer, C.U., Hvidberg, C.S., Steffensen, J.P., Sveinbjornsdottir, A.E., Jouzel, J., Bond, G., 1993. Evidence for general instability of past climate from a 250-kyr ice-core record. Nature 364, 218–220.

De Boer, A.M., Nof, D., 2004. The exhaust valve of the North Atlantic. Journal of Climate 17, 417–422.

Dyke, A.S., Dale, J.E., McNeely, R.N., 1996. Marine molluscs as indicators of environmental change in glaciated North America and Greenland during the last 18 000 years. Geographie physique et Quaternaire 50 (2), 125–184.

Ganopolski, A., Rahmstorf, S., 2001. Rapid changes of glacial climate simulated in a coupled climate model. Nature 409, 153–158.

Ganopolski, A., Rahmstorf, S., 2002. Abrupt glacial climate changes due to stochastic resonance. Physical Review Letters 88(3), 038501(1–4).

Giles, R., 1962. Theory and Problems of Fluid Mechanics and Hydraulics. McGraw-Hill, New York, 362pp.

Gill, A.E., 1982. Atmosphere–Ocean Dynamics. Academic Press, New York.

Godfrey, J.S., 1989. A sverdrup model of the depth-integrated flow for the ocean allowing for island circulations. Geophysical and Astrophysical Fluid Dynamics 45, 89–112.

Goosse, H., Campin, J.M., Fichefet, T., Deleersnijder, E., 1997. Sensitivity of a global ice–ocean model to the Bering Strait throughflow. Climate Dynamics 13, 349–358.

Hasumi, H., 2002. Sensitivity of the global thermohaline circulation to interbasin freshwater transport by the atmosphere and the Bering Strait throughflow. Journal of Climate 15, 2515–2526.

Haug, G.H., Tiedemann, R., 1998. Effect of the formation to the Isthmus of Panama on Atlantic Ocean thermohaline circulation. Nature 393, 673–676.

Hellerman, S., Rosenstein, M., 1983. Normal monthly wind stress over the world ocean with error estimates. Journal of Physical Oceanography 13 (7), 1093–1104.

Johnson, R.G., 2001. Last interglacial sea stands on Barbados and an early anomalous deglaciation timed by differential uplift. Journal of Geophysical Research 106 (C6), 11543–11551.

Keeling, R.F., 2002. On the freshwater forcing of the thermohaline circulation in the limit of low diapycnal mixing. Journal of Geophysical Research 107 (C7), 10.1029/2000JC000685.

Kukla, G.J., 2000. The last interglacial. Science 287, 987–988.

Labeyrie, L., 2000. Glacial climate instability. Science 290, 1905–1907.

Lambeck, K., Chappell, J., 2001. Sea level change through the last glacial cycle. Science 292, 679–686.

Ledwell, J.R., Watson, A.J., Law, C.S., 1993. Evidence for slow mixing across the pycnocline from an open-ocean tracer-release experiment. Nature 364, 701–703.

Manabe, S., Stouffer, R.J., 1993. Century-scale effects of increased atmospheric CO_2 on the ocean–atmosphere system. Nature 364, 215–218.

Marincovich, L., Gladenkov, A.Y., 1999. Evidence for an early opening of the Bering Strait. Nature 397, 149–151.

Marotzke, J., 2000. Abrupt climate change and thermohaline circulation: Mechanisms and predictability. Proceedings of the National Academy of Sciences 97 (4), 1347–1350.

Nilsson, J., Walin, G., 2001. Freshwater forcing as a booster of thermohaline circulation. Tellus 53A, 628–640.

Nof, D., 2000. Does the wind control the import and export of the South Atlantic. Journal of Physical Oceanography 30 (11), 2650–2667.

Nof, D., 2002. Is there a meridional overturning cell in the Pacific and Indian Oceans. Journal of Physical Oceanography 32 (6), 1947–1959.

Nof, D., Van Gorder, S., 2003. Did an open Panama Isthmus correspond to an invasion of Pacific water into the Atlantic? Journal of Physical Oceanography 33 (7), 1324–1336.

Park, Y.-G., 1999. The stability of thermohaline circulation in a two-box model. Journal of Physical Oceanography 29, 3101–3110.

Paul, A., Schulz, M., 2002. Holocene climate variability on centennial-to-millennial time scales: 2. internal and forced oscillations as possible causes. In: Wefer, G., Berger, W., Behre, K.-E., Jansen, E. (Eds.), Climate Development and History of the North Atlantic Realm. Springer, Berlin, pp. 55–73.

Peterson, L.C., Haug, G.H., Hughen, K.A., Rohl, U., 2000. Rapid changes in the hydrologic cycle of the tropical Atlantic during the last glacial. Science 290, 1947–1951.

Rahmstorf, S., Alley, R., 2002. Stochastic resonance in glacial climate. EOS 83 (12), 129–135.

Reid, J.L., 1961. On the temperature, salinity and density difference between the Atlantic and Pacific oceans in the ipper kilometer. Deep-Sea Research 7, 265–275.

Rioual, P., Andrieu-Ponel, V., Rietti-Shati, M., Battarbee, R.W., de Beaulieu, J.-L., Cheddadi, R., Reille, M., Svobodova, H., Shemesh, A., 2001. High-resolution record of climate stability in France during the last interglacial period. Nature 413, 293–296.

Romanova, V., Prange, M., Lohmann, G., 2004. Stability of the glacial thermohaline and its dependence on the background hydrological cycle. Climate Dynamics 22, 527–538.

Saravanan, R., McWilliams, J.C., 1995. Multiple equilibria, natural variability, and climate transitions in an idealized ocean–atmosphere model. Journal of Climate 8, 2296–2323.

Schäfer-Neth, C., Paul, A., 2000. Circulation of the glacial Atlantic: a synthesis of global and regional modeling. In: Schäfer, P., Ritzrau, W., Schlüter, M., Thiede, J. (Eds.), The Northern North Atlantic: A Changing Environment. Springer, Berlin, pp. 441–462.

Schiller, A., Mikolajewicz, U., Voss, R., 1997. The stability of the North Atlantic thermohaline circulation in a coupled ocean–atmosphere general circulation model. Climate Dynamics 13, 325–347.

Schmitt, R.W., Boden, P.S., Dorman, C.E., 1989. Evaporation minus precipitation and density fluxes for the North Atlantic. Journal of Physical Oceanography 19 (9), 1208–1221.

Schmittner, A., Yoshimori, M., Weaver, A.J., 2002. Instability of glacial climate in a model of the ocean–atmosphere–cryosphere system. Science 295, 1489–1493.

Shackleton, N.J., 1987. Oxygen isotopes, ice volume and sea level. Quaternary Science Reviews 6, 183–190.

Shaffer, G., Bendtsen, J., 1994. Role of the bering strait in controlling North Atlantic ocean circulation and climate. Nature 367, 354–357.

Shemesh, A., Rietti-Shati, M., Rioual, P., Battarbee, R., de Beaulieu, J.-L., Reille, M., Andrieu, V., Svobodova, H., 2001. An oxygen isotope record of lacustrine opal from a European Maar indicates climatic stability during the last interglacial. Geophysical Research Letters 28 (12), 2305–2308.

Stigebrandt, A., 1984. The North Pacific: a global-scale estuary. Journal of Physical Oceanography 14, 464–470.

Stocker, T.F., 1997. Influence of CO_2 emission rates on the stability of the thermohaline circulation. Nature 388, 862–865.

Stocker, T.F., 2000. Past and future reorganizations in the climate system. Quaternary Science Reviews 19, 301–319.

Stommel, H., 1961. Thermohaline convection with two stable regimes of flow. Tellus 13 (2), 224–230.

Tomczak, M., Godfrey, J.S., 1994. Regional Oceanogrpahy: An Introduction. Pergamon, Oxford.

Tziperman, E., Gildor, H., 2002. The stabilization of the thermohaline circulation by the temperature-precipitation feedback. Journal of Physical Oceanography 32, 2707–2714.

Wang, Z., Mysak, L.A., 2001. Ice sheet thermohaline circulation interactions in a simple climate model of intermediate complexity. Journal of Oceanography 57, 481–494.

Weijer, W., de Ruijter, W.P.M., Dijkstra, H.A., 2000. Stability of the Atlantic overturning circulation: competition between Bering Strait freshwater flux and Agulhas heat and salt sources. Journal of Physical Oceanography 31 (8), 2385–2402.

Yokoyama, Y., Lambeck, K., De Deckker, P., Johnston, P., Fifield, L.K., 2000. Timing of the Last Glacial Maximum from observed sea-level minima. Nature 406, 713–716.